Acta Biomaterialia 6 (2010) 2903–2910

Contents lists available at ScienceDirect

Acta Biomaterialia

journal homepage: www.elsevier.com/locate/actabiomat

Design of a self-cleaning thermoresponsive nanocomposite hydrogel membrane for implantable biosensors

R.M. Gant, A.A. Abraham, Y. Hou, B.M. Cummins, M.A. Grunlan *, G.L. Coté

Department of Biomedical Engineering, Mail Stop 3120, Texas A&M University, College Station, TX 77843, USA

ARTICLE INFO

Article history:
Received 30 November 2009
Received in revised form 20 January 2010
Accepted 26 January 2010
Available online 1 February 2010

Keywords:
Poly(*N*-isopropylacrylamide)
Hydrogel
Sensor membrane
Biofouling
Thermoresponsive

ABSTRACT

Following implantation of a biosensor, adhesion of proteins and cells and eventual fibrous encapsulation will limit analyte diffusion and impair sensor performance. A thermoresponsive nanocomposite hydrogel was developed as a self-cleaning biosensor membrane to minimize the effect of the host response and its utility for an optical glucose sensor, demonstrated here. It was previously reported that thermoresponsive nanocomposite hydrogels prepared from photopolymerization of an aqueous solution of *N*-isopropylacrylamide (NIPAAm) and polysiloxane colloidal nanoparticles released adhered cells with thermal cycling. However, poly(*N*-isopropylacrylamide) hydrogels exhibit a volume phase transition temperature (VPTT) of ~33–34 °C, which is below body temperature. Thus, the hydrogel would be in a collapsed state *in vivo*, which would ultimately limit diffusion of the target analyte (e.g., glucose) to the encapsulated sensor. In this study, the VPTT of the nanocomposite hydrogel was increased by introducing *N*-vinylpyrrolidone (NVP) as a comonomer, so that the hydrogel was in the swollen state *in vivo*. This thermoresponsive nanocomposite hydrogel was prepared by the photopolymerization of an aqueous solution of NIPAAm, NVP, and polysiloxane colloidal nanoparticles. In addition to a VPTT a few degrees above body temperature, the hydrogel also exhibited good mechanical strength, glucose diffusion, and *in vitro* cell release upon thermal cycling. Thus, this nanocomposite hydrogel may be useful as a biosensor membrane to minimize biofouling and extend the lifetime and efficiency of implantable glucose sensors and other biosensors.

1. Introduction

Optical biosensing techniques are advantageous because, after initial implantation, they can be used for continuous, non-invasive analyte detection. However, in order for an implanted sensor to perform well over time, the biological host response must be minimized so that the analyte diffusion and signal propagation will not be impaired. Even materials that are considered biocompatible can form tissue capsules on the surface of an implant. Depending on factors such as the physical properties of the material, size of the implant and implantation location, the fibrous encapsulation can range in size from ~0.05 to 1.5 mm [1,2]. The capsule could alter detected analyte levels by limiting diffusion to the sensor and by changing local analyte concentrations via metabolic reactions [3]. The optical signal could also be hindered by the additional light scatter and absorption.

Cross-linked thermoresponsive hydrogels reversibly switch from a hydrophilic, swollen state to a hydrophobic, deswollen state when heated above the volume phase transition temperature (VPTT) [4]. Thermal modulation of poly(*N*-isopropylacrylamide) (PNIPAAm) hydrogels has been used to release cell sheets from culture dishes without the use of potentially damaging enzymes or chelating agents [5–7]. It is anticipated that the cell-releasing behavior of PNIPAAm hydrogels may be used *in vivo* to minimize membrane biofouling of implanted sensors. The present authors previously reported a thermoresponsive nanocomposite hydrogel composed of a PNIPAAm hydrogel matrix and polysiloxane colloidal nanoparticles which released adhered cells upon thermal cycling [8]. However, the VPTT of these hydrogels is ~33–34 °C, which is below body temperature. Thus, when implanted in the body, the hydrogel would be in a deswollen state which would inhibit target analyte diffusion to the encapsulated sensor. Raising the VPTT of the thermoresponsive nanocomposite hydrogel to just above body temperature would render it in the swollen state *in vivo* to improve glucose diffusion and ultimately enhance biosensor efficiency. Furthermore, application of heat to deswell the membrane may be used to remove adhered proteins and cells.

In order to tailor the VPTT of the nanocomposite hydrogel, the precise body temperature in the targeted location for the biosensor must be considered. The normal body temperature of a human depends on many factors such as gender, race, activity level, fluid

* Corresponding author. Tel.: +1 979 8452406; fax: +1 979 8454450.
E-mail address: mgrunlan@tamu.edu (M.A. Grunlan).

1742-7061/$ - see front matter © 2010 Acta Materialia Inc. Published by Elsevier Ltd. All rights reserved.
doi:10.1016/j.actbio.2010.01.039

consumption and time of day. The average core body temperature for healthy adult humans at rest in thermoneutral conditions (i.e., when the body temperature is controlled without shivering or sweating) is ~36.8 ± 0.4 °C [9,10]. This internal body temperature is maintained within ~2 °C despite large variations in ambient temperature. Hardy et al. showed that, when temperatures were varied from 22 to 35 °C, subject core temperatures were relatively stable, while skin temperatures changed dramatically, especially at lower ambient temperatures [11]. The rate at which heat is transferred from the surface of the skin to the environment depends on the temperature difference between the two and the thermal conductivity of the surrounding medium [9].

Temperature variation occurs throughout the body because of differing geometry and material inhomogeneity [12]. An implanted optical sensor would optimally be located close to the surface of the tissue in order to minimize the optical signal path length. Therefore, it is likely to be strongly influenced by the environmental temperature, as more superficial tissues are more affected by imposed thermal stresses than deeper tissues are [13]. For glucose sensing described herein, the sensor is designed to be implanted in the subcutaneous tissue on the underside of the forearm. The inner temperature of the forearm has been determined as 35.5 °C, but this maximum temperature was measured at a depth of 4 cm, near the center of the arm [12]. At an ambient temperature of 23 °C, the forearm surface temperature has been found to range from 29.4 °C on the lateral side to 31.4 °C on the ventral surface [14]. If the sensor is implanted just under the surface of the skin, its average normal temperature is likely to be several degrees below 35.5 °C. Thus, in this study, body temperature at the site of the implanted glucose biosensor is considered to be ~35 °C.

The VPTT of PNIPAAm-based hydrogels is known to increase generally with copolymerization of *N*-isopropylacrylamide (NIPAAm) with hydrophilic comonomers [15,16]. In this study, the VPTT of the nanocomposite hydrogel was increased by introducing *N*-vinylpyrrolidone (NVP) as a hydrophilic comonomer. Because the VPTT of the resulting hydrogel is above body temperature, it will exist in the swollen state *in vivo* to permit diffusion of glucose. The "self-cleaning" mechanism of the hydrogel sensor membrane was activated by cyclically raising the temperature above the VPTT and subsequently allowing it to cool to body temperature. Because thermal damage may occur to the surrounding tissue above 41.6–42 °C, the temperature did not exceed this during heating [17].

2. Materials and methods

2.1. Materials

NIPAAm, NVP, potassium persulfate, ammonium hydroxide, sodium chloride, sodium phosphate, potassium phosphate, hydrochloric acid, and sodium hydroxide were purchased from Sigma–Aldrich (St. Louis, MO). Potassium chloride was purchased from Fisher Scientific (Pittsburgh, PA). 1-[(2-Hydroxyethoxy)-phenyl]-2-hydroxy-2-methyl-1-propane-1-one (Irgacure-2959) was obtained from Ciba Specialty Chemicals (Tarrytown, NY). *N*,*N*′-methylene bis-acrylamide (BIS) was purchased from Acros Organics (Geel, Belgium). Octamethylcyclotetrasiloxane (D_4) and 1,3,5,7-tetramethyl-1,3,5,7-tetravinylcyclotetrasiloxane (D_4^{Vi}) came from Gelest, and dodecylbenzenesulfonic acid (BIO-SOFT®) came from Stepan (Northfield, IL). The Slide-A-Lyzer dialysis cassette (MWCO 10,000) was obtained from Pierce (Rockford, IL). Aqueous experiments were performed with deionized (DI) water with a resistance of 18 MΩ cm (Millipore, Billerica, MA). The pH of the 1× phosphate buffered saline (PBS) solution was adjusted to 7.4 using 1 M HCl and 1 M NaOH and verified with a pH meter (420 A+, Orion; electrode 5990-30, Cole-Parmer, Vernon Hills, IL).

2.2. Hydrogel sensor membrane fabrication

Thermoresponsive nanocomposite hydrogels based on PNIPAAm and polysiloxane colloidal nanoparticles were prepared as previously reported by Hou et al. [18]. Polysiloxane nanoparticles had an average diameter of 219 nm, with particles ranging in size from 106 to 531 nm. In this study, hydrogels were prepared from precursor solutions composed of DI water, 8–14 wt.% NIPAAm monomer, 1–2 wt.% NVP comonomer, 0.2–1 wt.% BIS cross-linker, 1 wt.% Irgacure-2959 photoinitiator, and 1 wt.% polysiloxane colloidal nanoparticles. Values for NIPAAm, NVP, BIS, and Irgacure were weight percentage based on total precursor solution weight, while the nanoparticles were weight percentage solids of nanoparticles based on total precursor solution weight. The solution was injected between two glass microscope slides (75 × 50 mm) separated by spacers 1 mm thick. The mold was submerged in an ice water bath (~7 °C) and exposed to UV light for 10 min (UVP UV-Transilluminator, 6 mW cm^{-2}, λ_{peak} = 365 nm). The hydrogel sheets were removed from the mold, rinsed with DI water and soaked for at least 48 h in DI water or PBS at room temperature (RT) to remove impurities and allow for adequate hydration prior to use. After soaking the hydrogels, there was no detectable weight loss by gravimetric measurement, thereby indicating that the sol content was quite small. From these hydrogel sheets, square slabs were cut using a clean razor blade for morphological, VPTT, equilibrium swelling, diffusion and cell adhesion tests. Circular discs of a specific diameter were punched from hydrogel sheets for swelling/deswelling kinetic studies and compression testing.

For tensile tests, hydrogels were prepared with a ring geometry. First, hydrogels were prepared in a hollow tube geometry with a double-walled tubular mold composed of an inner glass mandrel (diameter 3 mm) and an outer glass cylinder (diameter 7.5 mm). The tubular mold was filled with the precursor solution and cured while submerged in an ice water bath (~7 °C) for 20 min under constant rotation such that each surface point of the mold received equal UV intensity and exposure time. The hydrogel tube was removed from the mold and similarly purified as above by rinsing and soaking in PBS. Cutting the resulting hydrogel tube into pieces ~3 mm wide afforded hydrogel ring specimens. For each of these tests, enough samples were prepared to perform measurements in triplicate.

2.3. Morphological characterization

Hydrogel specimens were subsequently maintained at either 4 °C (below VPTT) or 50 °C (above VPTT) in PBS for 24 h to promote swelling or deswelling, respectively. They were subsequently flash frozen in liquid N_2 to preserve morphology and freeze-dried in a lyophilizer (Labconco CentriVap Gel Dryer System, Kansas City, MO) for 6 h at −40 °C. Cross sections were sputter-coated with gold and visualized by field emission scanning electron microscopy (FE-SEM; Quanta 600 FE-SEM, FEI, Hillsboro, OR).

2.4. Measurement of VPTT

The VPTT of the hydrogels was determined using differential scanning calorimetry (DSC; TA Instruments Q100, New Castle, DE). After soaking in either DI water or PBS at RT, the hydrogel specimens were blotted with filter paper and sealed in a hermetic pan. After cooling to −50 °C, the temperature was increased to 50 °C at a rate of 3 °C min^{-1} for each cycle. The resulting exothermic phase transition peak is characterized by the temperature at the onset of the exotherm (T_o) and the peak temperature of the exotherm (T_{max}). Data reported are from the second cycle.

2.5. Measurement of equilibrium swelling

For equilibrium swelling measurements, hydrogel slabs of constant dimension (1 cm × 1 cm × 1 mm) were prepared as above. Hydrogel equilibrium swelling ratio is defined as: swelling ratio = $(W_s - W_d)/W_d$, where W_s is the weight of the water-swollen hydrogel at a certain temperature, and W_d is the weight of the oven-dried hydrogel (40 °C, 24 h). Each square was sealed inside a vial containing 20 mL DI water or PBS, immersed in a temperature controlled water bath for 24 h at the designated temperature (10–50 °C), removed, blotted with filter paper to remove surface water, and weighed (W_s).

2.6. Measurement of swelling/deswelling kinetics

For kinetic swelling/deswelling measurements, hydrogel discs of constant dimension (diameter 8 mm, thickness 1 mm) were prepared as above. The hydrogel discs were maintained in PBS at either 35 or 39 °C for 24 h and then placed in PBS at the opposite temperature at time zero. The change in swelling was measured by removing the discs from the solution and immediately measuring the diameter with a digital caliper.

2.7. Measurement of glucose diffusion

The diffusion through the hydrogels previously maintained in PBS was measured using glucose as an example analyte. The hydrogel slabs (1 cm × 1 cm × 1 mm) were placed in a side-by-side diffusion cell (PermeGear, Bethlehem, PA) with glucose solution (1000 mg dL^{-1}) in the donor chamber and DI water in the receptor chamber. The solutions were stirred to provide even concentrations, and a water jacket was used to maintain a consistent temperature. Samples were taken every 20 min from the receptor chamber, and the glucose concentration was measured using a YSI 2700 Select Biochemistry Analyzer (YSI Incorporated, Yellow Springs, OH). Average hydrogel slab thicknesses were measured on a DMA Q800 (TA Instruments, New Castle, DE) and the diffusion coefficients were calculated using Fick's second law of diffusion.

2.8. Dynamic mechanical analysis

Dynamic mechanical analysis (DMA) was performed in the compression mode using a DMA Q800 (TA Instruments, New Castle, DE) equipped with a parallel-plate compression clamp with a diameter of 40 mm (bottom) and 15 mm (top). Swollen hydrogel discs of constant dimension (diameter 13 mm, thickness 1 mm) were punched from a hydrogel sheet maintained in PBS. Each disc was clamped between the parallel plates, and silicone oil was placed around the exposed edges to prevent dehydration. The hydrogel discs were allowed to equilibrate for 5 min at either 35 or 39 °C and were then tested in multi-frequency-strain mode (1–100 Hz).

2.9. Tensile tests

Tensile tests of hydrogels ring specimens were performed using a TA Instruments DMA Q800 operating in tension mode. Specimens with ring geometry were prepared by cutting a portion from a hydrogel tube produced from the double wall tubular mold (ID = 3 mm, OD = 7.5 mm) as above. Individual rings (width ~3 mm) were cut from the central portion of the appropriate hydrogel tube using a clean razor blade, and sample dimensions were measured with a digital caliper. Each hydrogel ring was blotted with filter paper and loaded onto custom aluminum bars gripped directly into DMA tension clamps so that the upper and lower bars were located inside the ring. Samples were subjected to a constant strain (1 mm min^{-1}) until they broke at the center of one side of the ring. Stress was calculated from the measured force divided by the cross-sectional area of two rectangles with sides equal to the width and wall thickness of the ring. The gauge length corresponded to the outer diameter of the ring less the wall thickness. The following parameters were determined: (1) tensile modulus; (2) ultimate tensile strength (UTS); and (3) percentage strain at break. The tensile modulus was obtained from the slope of the linear part of the stress–strain curve. The UTS represents the maximum stress prior to failure. Strain was calculated from the measured displacement divided by the gauge length. Results reported are the average result of three specimens cut from the central portion of the same hydrogel tube.

2.10. Measurement of "self-cleaning" properties

Hydrogels and polystyrene controls were sterilized by exposure to 70% ethanol for 45 min. The samples were then washed three times with sterile Dulbecco's PBS for 30 min each and placed in DMEM overnight. The samples were inoculated with GFP-H2B 3T3 mouse fibroblast cells maintained in DMEM with 10% fetal calf serum and antibiotics. A non-thermoresponsive polystyrene control and a nanocomposite hydrogel were maintained at 35 °C, while a duplicate set was cycled between 35 and 39 °C every hour. The average rate of heating to 39 °C was 0.63 °C min^{-1} and cooling to 35 °C was 0.49 °C min^{-1}. Three hydrogel slabs of each material and group were removed daily and imaged (Nikon Eclipse TE 2000-S) to obtain a cell count. Both constant and variable temperature specimens were evaluated over a period of 7 days.

3. Results and discussion

3.1. Material design

Thermoresponsive nanocomposite hydrogels were designed to have a VPTT slightly above body temperature, so that the hydrogels would be swollen in the resting state *in vivo* in order to maximize diffusion of glucose. There are several methods to alter the VPTT, including adjusting the pH or adding surfactants, both of which would be physiologically infeasible. [19,20]. The other widely used method is the introduction of a comonomer [15,16,21]. In order to raise the VPTT, a hydrophilic comonomer, NVP, was added to the hydrogel precursor solution. In addition to the design constraint of the VPTT, the other components of the hydrogel were also considered with regard to impact on swelling, diffusion and mechanical strength. In general, hydrogel swelling decreases with total monomer concentration in the precursor solution as well as with higher cross-linker levels. Lower levels of swelling are expected to increase mechanical strength but diminish diffusion. A design of experiments analysis was performed using JMP statistical software to optimize the formula by varying the hydrogel components as described in Table 1.

Each potential combination of components was tested based on maximum swelling ratio, diffusion and mechanical strength to predict the most desirable formula for use in the temperature range of interest. The optimal composition was determined as 9 wt.% NIPAAm monomer, 1 wt.% NVP comonomer, 87.8 wt.% water,

Table 1
Percentage range of the three components.

Component	Range (wt.%)
Total monomer	10–15
NVP	1–2
BIS	0.2–1

0.2 wt.% BIS cross-linker, 1 wt.% polysiloxane nanoparticles (weight percentage solids of nanoparticles with respect to total precursor solution weight), and 1 wt.% Irgacure photoinitiator (all weight percentage based on total precursor solution weight).

3.2. Material characterization

The self-cleaning mechanism of the nanocomposite hydrogel will be induced with cyclical heating above the VPTT and cooling below the VPTT to cause deswelling and swelling, respectively. In addition to the physical change in the hydrogel, concomitant changes in surface hydrophilicity with thermal cycling also contribute to cell release. Because the hydrogels were photochemically cured at a low temperature (~7 °C), homogeneous rather than heterogeneous hydrogels were expected to be formed as previously reported [22–25]. In order to view the morphological differences between the swollen and deswollen states, the hydrogels were maintained in PBS either below the VPTT (4 °C) or above the VPTT (50 °C) and then lyophilized to preserve the hydrogel structure and volume [26,27]. SEM images were then acquired, as shown in Fig. 1. Hydrogels maintained below the VPTT (swollen state) exhibited a homogeneous, expanded network, whereas those maintained above the VPTT (deswollen state) were homogeneous but substantially contracted.

Characterization of the VPTT of PNIPAAm hydrogels has been typically conducted on those prepared with and/or soaked in DI water. However, upon implantation as a sensor membrane, the hydrogel will be subjected to a physiological environment. Thus, it is important to analyze the functionality of an implantable sensor under physiological conditions, particularly with respect to pH and salinity. Designed to be implanted in the subcutaneous tissue, the sensor will be bathed in interstitial fluid. The human body can control the pH of blood and interstitial fluid to within a tenth of a pH unit of 7.4 [28]. Since the pH of DI water is ~7, a slightly more basic solution should be used for more accurate testing. PNIPAAm has been considered a pH-sensitive material [29,30]. However, other work supports the idea that the changes seen are in fact due to other factors such as a copolymer or the salts used in the preparation of the pH buffer solutions, and not necessarily to the change in pH [19,31]. The VPTT of PNIPAAm can be changed with the addition of various salts by a salting out effect which causes a decrease in VPTT [19,20,32,33]. The type of salt, valence, size of the anions and the concentration have a strong influence on the effect. The salting out may be due to a combination of several effects, including changes in the water structure in the hydration layer surrounding the polymer and changes in the interactions between the polymer and the solvent. The addition of electrolytes changes the normal hydrogen bonded water structure, disrupting the highly oriented water molecules, resulting in an increase in the hydrophobicity of the PNIPAAm and a subsequent decrease in the VPTT [20].

Given the known effects of pH, salts and electrolytes on the VPTT of PNIPAAm, the present studies were conducted with nanocomposite hydrogel samples that were maintained in both DI water and PBS for 48 h prior to specific tests. The impact of PBS on the VPTT is shown in Table 2. The VPTT was characterized by both the onset (T_o) or the maximum temperature (T_{max}) of the endothermic peak [16,22]. Hydrogels saturated in PBS displayed a lower VPTT in terms of T_o and T_{max} values. As expected, the addition of the hydrophilic comonomer NVP raised the VPTT. Thus, at physiological conditions, the nanocomposite hydrogel prepared with NVP is expected to exhibit a VPTT above body temperature. This will render the hydrogel in the hydrated, swollen state when implanted in the body for enhanced diffusion of glucose to the encapsulated sensor. Cyclical heating to 39 °C followed by cooling to body temperature will cause deswelling and swelling, respectively.

3.3. Equilibrium swelling

The extent of swelling and deswelling of the hydrogels was determined via equilibrium swelling measurements from 10 to 50 °C in both DI water and in PBS. As was seen in the DSC measurements of VPTT, Fig. 2 shows that the VPTT occurred at slightly lower temperatures for hydrogels soaked in PBS vs in DI water, and NVP increased the VPTT. Upon implantation, greater swelling of the hydrogel membrane would enhance diffusion in the resting state at 35 °C. The self-cleaning mechanism of the hydrogel will be activated by heating to 39 °C to cause hydrogel deswelling and release of adsorbed cells. At ~39 °C, the hydrogel containing NVP and in PBS (A) produced the most significant deswollen state. The extent of deswelling or the net change in swelling from 35 to 39 °C of hydrogel A was as significant as in water (B) and more substantial than for the hydrogel without NVP (C). The large extent of deswelling is expected to maximize the self-cleaning mechanism.

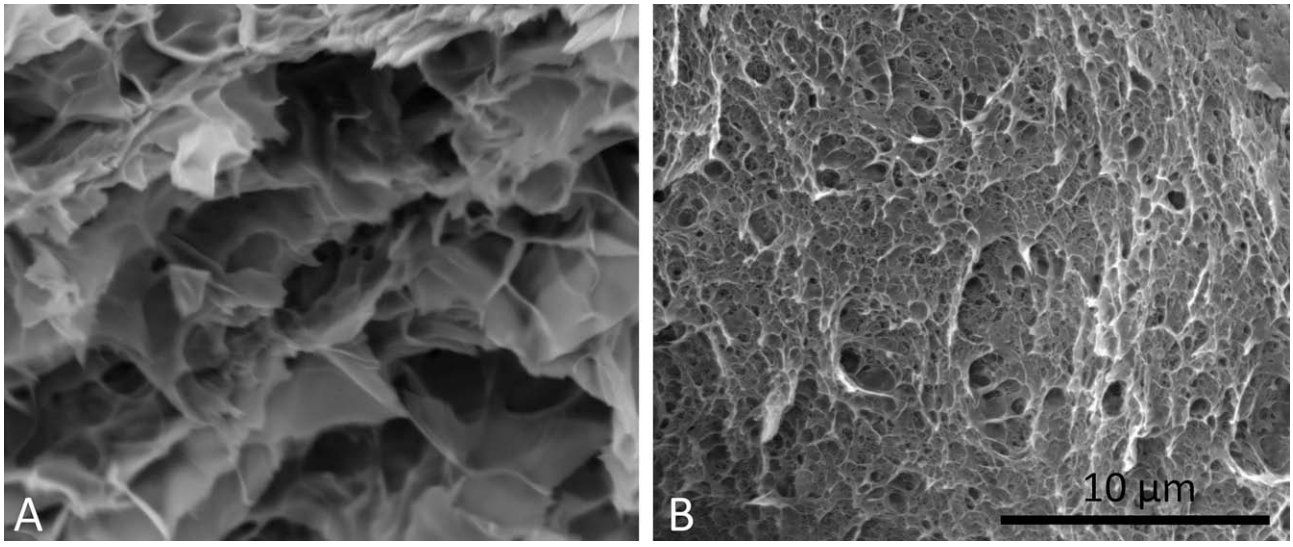

Fig. 1. SEM micrographs of hydrogels displaying (A) swollen morphology after conditioning below the VPTT at 4 °C and (B) deswollen morphology after conditioning above the VPTT at 50 °C.

Table 2
VPTT of hydrogels with and without comonomer NVP in either DI water or PBS.

	T_o (°C)	T_{max} (°C)
(A) With NVP, in PBS	34.6 ± 0.7	37.4 ± 1.5
(B) With NVP, in water	38.1 ± 0.3	41.8 ± 0.1
(C) Without NVP, in PBS	30.4 ± 1.8	31.7 ± 1.7
(D) Without NVP, in water	32.8 ± 0.3	34.9 ± 0.1

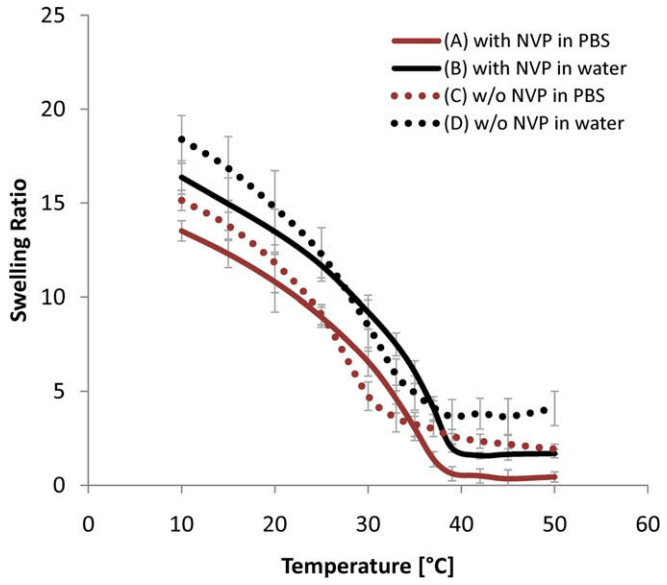

Fig. 2. Equilibrium swelling ratios as a function of temperature for (A) hydrogel with NVP in PBS, (B) hydrogel with NVP in water, (C) hydrogel without NVP comonomer in PBS, and (D) hydrogels without NVP in water.

3.4. Swelling and deswelling kinetics

Deswelling and swelling kinetics were studied for hydrogel A (with NVP) by measuring hydrogel disc diameter at regular time intervals while heating hydrogel discs in PBS from 35 °C (<VPTT) to 39 °C (>VPTT) and cooling from 39 to 35 °C, respectively (Fig. 3). Whereas swelling began rapidly upon cooling, deswelling appeared to be slower. This may be in part due to the limitations of the measurement; the diameters of the hydrogels during deswelling may have increased during the physical measurement at RT due to reswelling, even though each measurement lasted only a few seconds. In additional, formation of a surface skin during deswelling may limit water expulsion from the bulk [34,35]. Enhancing deswelling may be effected with modifications to the polymerization conditions, poration and freeze-drying if a quicker transition is necessary [27,36–38].

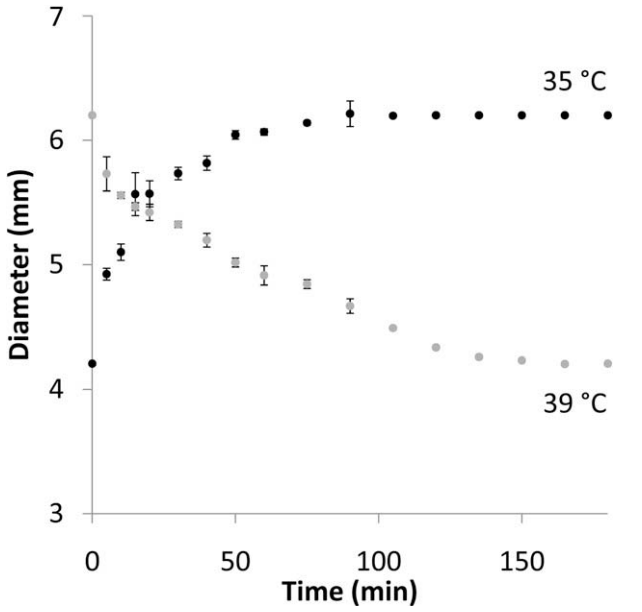

Fig. 3. For hydrogel A (with NVP in PBS), kinetics of swelling (●) upon cooling to 35 °C and deswelling (○) upon heating to 39 °C.

3.5. Glucose diffusion

The diffusion through the hydrogels was studied using glucose as an example analyte, as it is of particular interest for the development of implantable sensors. A side-by-side diffusion cell was used to monitor the glucose transport through the gels, and Fick's second law of diffusion was used to calculate the diffusion coefficients for each case.

$$\frac{\partial c}{\partial t} = D\frac{\partial^2 c}{\partial x^2}$$

where c is the concentration in the hydrogel, t is time, D is the diffusion coefficient, and x is distance [39–41]. Assuming that the chambers are well mixed by stirbars, and concentrations do not vary between the gel surface and the bulk fluid, this can be solved to:

$$Q_t = \frac{ADC_1}{l}\left(t - \frac{l^2}{6D}\right)$$

where Q_t is the total amount of glucose transferred through the gel until time t, A is gel area, C_1 is the glucose concentration in the donor chamber, and l is gel thickness.

Table 3 shows the effect of temperature on the diffusion coefficients of hydrogels created with and without the comonomer NVP. At 30 °C, both hydrogels are below the VPTT, and the swollen nature of the hydrogel permits similar glucose diffusion. At temperatures above the VPTT, the hydrogel collapses into a deswollen state to inhibit glucose diffusion. At 35 °C (body temperature), the hydrogel prepared with NVP (A) is below its VPTT, whereas the hydrogel prepared without NVP (C) is above its VPTT. Thus, glucose diffusion is greater for the former hydrogel (A). Not until hydrogel (A) is heated above 39 °C is a substantial decrease in glucose diffusion observed. Thus, upon implantation, the hydrogel prepared with NVP would permit better glucose diffusion in the resting state when not subjected to thermal heating to self-clean the surface. Glucose diffusion through the dermal layer of skin has been previously measured as 2.64×10^{-6} and as 0.075×10^{-6} $cm^2\ s^{-1}$ through the epidermis [42]. Though the hydrogels with NVP experience a slight decrease in diffusion rate at the activated temperature, it appears to be still within a useable range.

Table 3
Effect of temperature on diffusion coefficients of hydrogels with and without the comonomer NVP ($cm^2\ s^{-1}$) in PBS.

Temperature (°C)	Without NVP (C) (VPTT ≈ 31 °C)	With NVP (A) (VPTT ≈ 38 °C)
30	1.09×10^{-6}	1.33×10^{-6}
35	0.193×10^{-6}	1.24×10^{-6}
39	0.0483×10^{-6}	0.785×10^{-6}

3.6. Mechanical properties

Mechanical robustness is desired for an implanted sensor membrane to permit insertion, removal and integrity during residence in the body. Although swelling enhances diffusion, it also leads to reduced mechanical strength. Many methods for improving hydrogel strength do so by reducing swelling [43]. For instance, PNIPAAm hydrogels formed at $T < \sim 20$ °C are morphologically homogeneous, whereas those formed at higher temperatures are heterogeneous [23,24,44]. At $T > \sim 20$ °C, newly formed insoluble PNIPAAm chains phase separate, such that subsequent cross-linking leads to the formation of a macroscopic network of loosely interconnected highly cross-linked polymer-rich domains and lightly cross-linked polymer-poor domains. Heterogeneous PNIPAAm hydrogels display greater swelling, but are mechanically weaker compared with the corresponding homogeneous hydrogel. To maintain mechanical integrity, homogeneous hydrogels were prepared for this study. In addition, polysiloxane colloidal nanoparticles were incorporated to improve the mechanical properties of the nanocomposite hydrogels without affecting the VPTT or reducing swelling [18]. For compression and tensile tests, measures were taken to avoid dehydration of the specimens, which would falsely increase mechanical rigidity and strength. Mechanical tests were performed at 35 and 39 °C on hydrogel A (i.e., prepared with NVP and maintained in PBS) to determine the change in mechanical properties in a swollen vs deswollen state, respectively.

The storage modulus (G') is related to the stiffness or rigidity of the material [45]. At higher temperatures, less water is present in the hydrogel matrix, resulting in a stiffer, more compact structure. As expected, the deswollen hydrogel at 39 °C exhibited a higher G' at all frequencies vs the swollen hydrogel at 35 °C due to the lower water content of the former (Fig. 4). The tensile modulus, UTS and percentage strain at break also increased for the deswollen hydrogel at 39 °C (Table 4). This change in hydrogel stiffness during thermal cycling may contribute to cell detachment. Materials with modulus values much greater than the surrounding tissue are known to cause local irritation and a greater host response [46]. Though mechanical properties of specialized connective tissue such as bone, cartilage and tendon have been extensively studied, much less information is available regarding the behavior of loose connective tissue in humans. Iatridis et al. found the equilibrium tensile modulus of subcutaneous rat tissue to be 2.75 kPa [47]. Thus, the modulus of the hydrogel is similar to soft tissue and would be expected to minimize local irritation.

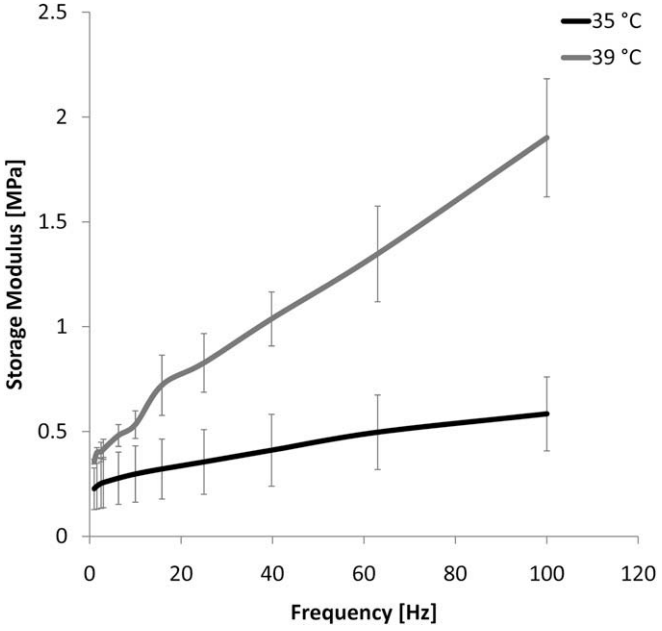

Fig. 4. Storage modulus (G') of hydrogel A at 35 and 39 °C measured in compression mode.

Table 4
Tensile properties of hydrogel (A).

	35 °C	39 °C
Modulus (kPa)	2.0 ± 0.4	8.5 ± 1.1
UTS (kPa)	89.2 ± 27.9	353.7 ± 46.2
% Strain at break	68.3 ± 7.1	78.8 ± 5.8

3.7. "Self-cleaning"

In order to determine the effect of a variable thermal environment on cell adhesion, hydrogel A and polystyrene control samples were inoculated with GFP-labeled H2B 3T3 mouse fibroblast cells and exposed to either a constant temperature of 35 °C or cycled between 35 and 39 °C every hour. Fig. 5 shows that, for both polystyrene control and hydrogel A samples maintained at 35 °C, the number of cells increased throughout the week. Because of the tendency of cells to adhere to hydrophobic surfaces, the hydrophobic polystyrene controls exhibited more cell attachment at the end of the week compared with the hydrophilic hydrogel when maintained at 35 °C. With thermal cycling, the polystyrene control also exhibited increasing cell numbers with time, showing that variations in the temperature did not cause cell death. The slight decrease in cell count between days 5 and 6 is attributed to cells that may have been disturbed when the used cell culture media was exchanged for fresh DMEM. The time required to completely detach cells from PNIPAAm films depends on cell types and the physiochemical properties of the specific hydrogel [48]. This thermal cycling schedule of the hydrogel was effective at limiting cell adhesion, demonstrating the possible utility of this system as a self-cleaning sensor membrane for glucose biosensors.

4. Conclusions

A thermoresponsive nanocomposite hydrogel was developed as a self-cleaning membrane to control the host response and extend the lifetime and efficiency of implanted biosensors. The swelling, diffusion and mechanical strength were optimized for *in vivo* conditions. By incorporating a hydrophilic comonomer, NVP, the VPTT was increased so that the hydrogel would exist in the swollen state at body temperature, which would permit increased diffusion of the target analyte (e.g., glucose) to the enclosed sensor. The "self-cleaning" mechanism of the hydrogel membrane is activated by cyclically raising the temperature above the VPTT and subsequently cooling to body temperature. Even though the diffusion rate is lower in the "active" state, the addition of NVP significantly improves glucose transfer. During deswelling, the dynamic compression modulus (G') as well as tensile modulus increased. This increase in hydrogel rigidity should contribute to diminished adhesion of cells in addition to the effects due to the changes in surface hydrophilicity. Though further research is needed to determine the necessary duty cycle to promote optimal diffusion while limiting cell adhesion and to assess *in vivo* functionality, the *in vitro* cell adhesion rates are promising. Over a period of 7 days, it was found that hydrogels that were exposed to thermal cycling had very low levels of cell attachment throughout the course of the study.

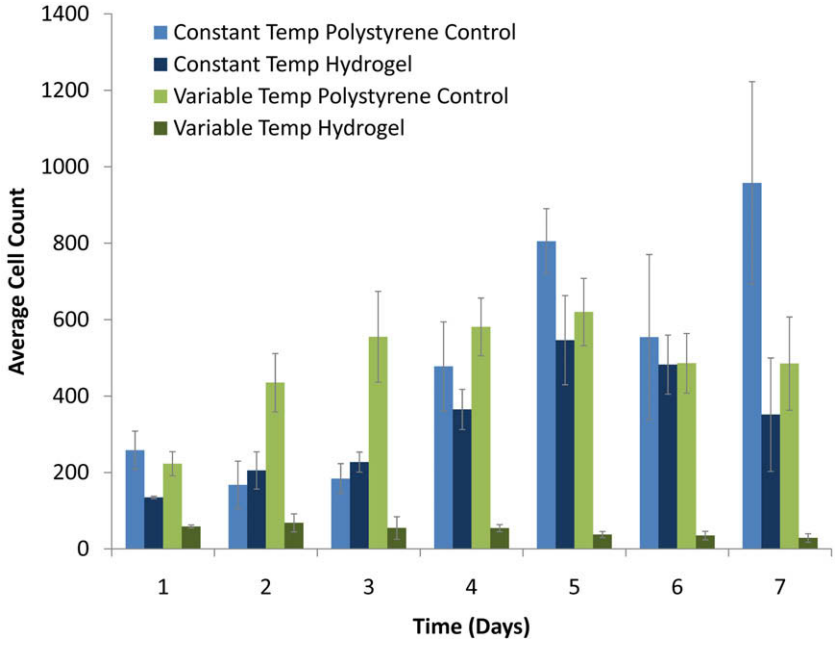

Fig. 5. Cell adhesion over time for hydrogels A and polystyrene controls maintained at either constant or variable temperatures.

Acknowledgments

Funding from the NIH/NIDDK (1R21DK082930-01A1) is gratefully acknowledged. FE-SEM acquisition was supported by the National Science Foundation (DBI-0116835), the Vice President for Research (VPR) Office, and the Texas Engineering Experiment Station (TEES).

Appendix A. Figures with essential colour discrimination

Certain figures in this article, particularly Figs. 2 and 5, are difficult to interpret in black and white. The full colour images can be found in the on-line version, at doi: 10.1016/j.actbio.2010.01.039.

References

[1] Shtilman MI. Polymeric biomaterials. Part I: Polymer implants. Boston: VSP; 2003.
[2] Zaikov GE, editor. Polymers in medicine. Commack, NY: Nova Science; 1998.
[3] Frost M, Meyerhoff ME. In vivo chemical sensors: tackling biocompatibility. Anal Chem 2006;78(21):7370–7.
[4] Freitag R, editor. Synthetic polymers for biotechnology and medicine. Austin, TX: Eurekah; 2003.
[5] Yamada N, Okano T, Sakai H, Karikusa F, Sawasaki Y, Sakurai Y. Thermo-responsive polymeric surfaces; control of attachment and detachment of cultured cells. Makromol Chem Rapid Commun 1990;11:571–6.
[6] Yamato M, Utsumi M, Kushida A, Konno C, Kikuchi A, Okano T. Thermo-responsive culture dishes allow the intact harvest of multilayered keratinocyte sheets without dispase by reducing temperature. Tissue Eng 2001;7(4):473–80.
[7] Takezawa T, Mori Y, Yoshizato K. Cell culture on a thermo-responsive polymer surface. Nat Biotech 1990;8(9):854–6.
[8] Gant RM, Hou Y, Grunlan MA, Cote GL. Development of a self-cleaning sensor membrane for implantable biosensors. J Biomed Mater Res A 2008;90(3):695–701.
[9] Blatteis CM, editor. Physiology and pathophysiology of temperature regulation. River Edge, NJ: World Scientific; 1998.
[10] Savage MV, Brengelmann GL. Control of skin blood flow in the neutral zone of human body temperature regulation. J Appl Physiol 1996;80(4):1249–57.
[11] Hardy JD, Du Bois EF, Soderstrom GF. Basal metabolism, radiation, convection and vaporization at temperatures of 22 to 35 °C: six figures. J Nutr 1938;15(5):477–97.
[12] Werner J, Buse M. Temperature profiles with respect to inhomogeneity and geometry of the human body. J Appl Physiol 1988;65(3):1110–8.
[13] Ducharme MB, Tikuisis P. Forearm temperature profile during the transient phase of thermal stress. Eur J Appl Physiol 1992;64:395–401.
[14] Montgomery LD, Williams BA. Effect of ambient temperature on the thermal profile of the human forearm, hand, and fingers. Ann Biomed Eng 1976;4:209–19.
[15] Erbil C, Aras S, Uyanik N. Investigation of the effect of type and concentration of ionizable comonomer on the collapse behavior of *N*-isopropylacrylamide copolymer gels in water. J Polym Sci Polym Chem 1999;37:1847–55.
[16] Feil H, Bae YH, Feijen J, Kim SW. Effect of comonomer hydrophilicity and ionization on the lower critical solution temperature of *N*-isopropylacrylamide copolymers. Macromolecules 1993;26(10):2496–500.
[17] Bouchama A, Knochel JP. Heat stroke. N Engl J Med 2002;346(25):1978–88.
[18] Hou Y, Matthews AR, Smitherman AM, Bulick AS, Hahn MS, Hou H, et al. Thermoresponsive nanocomposite hydrogels with cell-releasing behavior. Biomaterials 2008;29(22):3175–84.
[19] Geever LM, Nugent MJD, Higginbotham CL. The effect of salts and pH buffered solutions on the phase transition temperature and swelling of thermoresponsive pseudogels based on *N*-isopropylacrylamide. J Mater Sci 2007;42:9845–54.
[20] Eeckman F, Amighi K, Moes AJ. Effect of some physiological and non-physiological compounds on the phase transition temperature of thermoresponsive polymers intended for oral controlled-drug delivery. Int J Pharm 2001;222:259–70.
[21] Stile RA, Burghardt WR, Healy KE. Synthesis and characterization of injectable poly(*N*-isopropylacrylamide)-based hydrogels that support tissue formation in vitro. Macromolecules 1999;32(22):7370–9.
[22] Singh D, Kuckling D, Choudhary V, Adler HJ, Koul V. Synthesis and characterization of poly(*N*-isopropylacrylamide) films by photopolymerization. Polym Adv Technol 2006;17(3):186–92.
[23] Sayil C, Okay O. The effect of preparation temperature on the swelling behavior of poly(*N*-isopropylacrylamide) gels. Polym Bull 2000;45(2):175–82.
[24] Kayaman N, Kazan D, Erarslan A, Okay O, Baysal BM. Structure and protein separation efficiency of poly(*N*-isopropylacrylamide) gels: effect of synthesis conditions. J Appl Polym Sci 1998;67(5):805–14.
[25] Ju XJ, Chu LY, Zhu XL, Hu L, Song H, Chen WM. Effects of internal microstructures of poly(*N*-isopropylacrylamide) hydrogels on thermo-responsive volume phase-transition and controlled-release characteristics. Smart Mater Struct 2006;15(6):1767–74.
[26] Bekiari V, Lianos P. Photophysical behavior of terpyridine–lanthanide ion complexes incorporated in a poly(*N*,*N*-dimethylacrylamide) hydrogel. Langmuir 2006;22:8602–6.
[27] Kato N, Gehrke SH. Microporous, fast response cellulose ether hydrogel prepared by freeze-drying. Colloid Surf B 2004;38(3–4):191–6.
[28] Campbell NA, Reece JB, Mitchell LG. Biology. Menlo Park, CA: Benjamin Cummings; 1999.
[29] Hobabi MR, Hassanzadeh D, Azarmi S, Entezami AA. Effect of synthesis method and buffer composition on the LCST of a smart copolymer of *N*-isopropylacrylamide and acrylic acid. Polym Adv Technol 2007;18:986–92.
[30] Pei Y, Chen J, Yang L, Shi L, Tao Q, Hui B, et al. The effect of pH on the LCST of poly(*N*-isopropylacrylamide) and poly(*N*-isopropylacrylamide-co-acrylic acid). J Biomater Sci Polym E 2004;15(5):585–94.
[31] Jones MS. Effect of pH on the lower critical solution temperatures of random copolymers of *N*-isopropylacrylamide and acrylic acid. Eur Polym J 1999;35(5):795–801.

[32] Liu X-M, Wang L-S, Wang L, Huang J, He C. The effect of salt and pH on the phase-transition behaviors of temperature-sensitive copolymers based on *N*-isopropylacrylamide. Biomaterials 2004;25(25):5659–66.
[33] Eeckman F, Moes AJ, Amighi K. Evaluation of a new controlled-drug delivery concept based on the use of thermoresponsive polymers. Int J Pharm 2002;241:113–25.
[34] Bae YH, Okano T, Hsu R, Kim SW. Thermo-sensitive polymers as on–off switches for drug release. Makromol Chem Rapid Commun 1987;8: 481–5.
[35] Zhang J-T, Bhat R, Jandt KD. Temperature-sensitive PVA/PNIPAAm semi-IPN hydrogels with enhanced responsive properties. Acta Biomater 2009;5:488–97.
[36] Lee W, Yen S. Thermoreversible hydrogels. XII. Effect of the polymerization conditions on the swelling behavior of the *N*-isopropylacrylamide gel. J Appl Polym Sci 2000;78:1604–11.
[37] Zhang XZ, Chu CC. Thermosensitive PNIPAAm cryogel with superfast and stable oscillatory properties. Chem Commun 2003;12:1446–7.
[38] Zhang XZ, Wang FJ, Chu CC. Thermoresponsive hydrogel with rapid response dynamics. J Mater Sci Mater Med 2003;14:451–5.
[39] Hannoun BJM, Stephanopoulos G. Diffusion coefficients of glucose and ethanol in cell-free and cell-occupied calcium alginate membranes. Biotechnol Bioeng 1986;28:829–35.
[40] Venancio A, Teixeira JA. Characterization of sugar diffusion coefficients in alginate membranes. Biotechnol Tech 1997;11(3):183–5.
[41] Teixeira JA, Mota M, Venancio A. Model identification and diffusion coefficients determination of glucose and malic acid in calcium alginate membranes. Chem Eng J 1994;56:B9–B14.
[42] Tuchin VV, editor. Handbook of optical sensing of glucose in biological fluids and tissues. Boca Raton, FL: CRC Press; 2009.
[43] Anseth KS, Bowman CN, Brannon-Peppas L. Mechanical properties of hydrogels and their experimental determination. Biomaterials 1996;17(17):1647–57.
[44] Takata S-i, Norisuye T, Shibayama M. Preparation temperature dependence and effects of hydrolysis on static inhomogeneities of poly(acrylamide) gels. Macromolecules 1999;32(12):3989–93.
[45] Wicks ZW, Jones FN, Pappas SP, editors. Organic coatings science and technology. New York: John Wiley; 1999.
[46] Ratner BD. A paradigm shift: biomaterials that heal. Polym Int 2007;56(10):1183–5.
[47] Iatridis JC, Wu J, Yandow JA, Langevin HM. Subcutaneous tissue mechanical behavior is linear and viscoelastic under uniaxial tension. Connect Tissue Res 2003;44:208–17.
[48] Chen B, Xu FJ, Fang N, Neoh KG, Kang ET, Chen WN, et al. Engineering cell de-adhesion dynamics on thermoresponsive poly(*N*-isopropylacrylamide). Acta Biomater 2008;4:218–29.